

Adaptive Control Barrier Functions with Vanishing Conservativeness Under Persistency of Excitation

Ricardo Gutierrez and Jesse B. Hoagg

Abstract—This article presents a closed-form adaptive control-barrier-function (CBF) approach for satisfying state constraints in systems with parametric uncertainty. This approach uses a sampled-data recursive-least-squares algorithm to estimate the unknown model parameters and construct a nonincreasing upper bound on the norm of the estimation error. Together, this estimate and upper bound are used to construct a CBF-based constraint that has nonincreasing conservativeness. Furthermore, if a persistency of excitation condition is satisfied, then the CBF-based constraint has vanishing conservativeness in the sense that the CBF-based constraint converges to the ideal constraint corresponding to the case where the uncertainty is known. In addition, the approach incorporates a monotonically improving estimate of the unknown model parameters—thus, this estimate can be effectively incorporated into a desired control law. We demonstrate constraint satisfaction and performance using 2 two numerical examples, namely, a nonlinear pendulum and a nonholonomic robot.

I. INTRODUCTION

Control systems are often required to respect state constraints (e.g., safety constraints) and achieve performance requirements such as minimizing a performance-based cost function or achieving tasks such as formation control [1]–[3], locomotion [4], or destination seeking performance subject to state constraints can be addressed using a variety of methods including model predictive control (e.g., [5]–[8] and barrier function approaches (e.g., [9]–[15]).

Control barrier functions (CBFs) are an approach to achieve forward invariance of a set that satisfies state constraints (e.g., safety) [10]. CBFs are commonly implemented as constraints in real-time optimization control methods (e.g., quadratic programs) in order to guarantee state-constraint satisfaction while also attempting to minimize a performance based cost [11]. The minimum-intervention problem is one common example, where a desired control u_d is designed to satisfy performance requirements but may not account for state constraints. Then, a control is generated that is as close as possible to u_d while satisfying a CBF constraint that guarantees state-constraint satisfaction. Examples of CBF applications include adaptive cruise control [11], [16], satellites [17], unmanned air vehicles [18], [19], and ground robots [20]–[24].

CBF methods are model based, and model uncertainty can lead to both state-constraint violations and poor performance.

R. Gutierrez and J. B. Hoagg are with the Department of Mechanical and Aerospace Engineering, University of Kentucky, Lexington, KY, USA. (e-mail: Ricardo.Gutierrez@uky.edu, jesse.hoagg@uky.edu).

R. Gutierrez is supported by the Fulbright-SENACYT Scholarship. This work is also supported in part by the National Science Foundation (1849213) and Air Force Office of Scientific Research (FA9550-20-1-0028).

Robust CBF methods such as [25], [26] address model uncertainty with respect to state-constraint satisfaction. However, robust CBF methods adopt worst-case bounds, which can lead to overly conservative system behavior. Moreover, robust CBFs do not specifically address performance degradation that typically arises due to model uncertainty. In other words, robust CBFs do not directly address that a desired control u_d may lead to poor performance because of model uncertainty.

As an alternative, adaptive CBF techniques can also address model uncertainty (e.g., [27]–[31]). For example, [27] presents an adaptive CBF for state-constraint satisfaction in the presence of model uncertainty. However, the approach in [27] can be conservative in the sense that the CBF constraint imposed for safety may be more conservative than needed. In [28], set-membership identification is combined with the basic approach of [27] to reduce conservativeness. Higher-order adaptive CBF methods are presented in [30].

This article presents an adaptive CBF approach that has 2 key features. First, the adaptive CBF for the state-constraint satisfaction is guaranteed to have nonincreasing conservativeness, that is, the conservativeness can be captured by a decreasing function of time. Moreover, the conservativeness vanishes in the case of persistency of excitation. Second, the approach incorporates an estimate of the unknown model parameters, where norm of the estimation error is guaranteed to be nonincreasing and vanishes in the case of persistency of excitation. Thus, the estimate of the unknown model parameters can be effectively incorporated into a desired control law. Together, these 2 features can help improve performance while ensuring state-constraint satisfaction.

II. NOTATION

Let $q : \mathbb{R}^n \rightarrow \mathbb{R}$ be continuously differentiable. Then, $q' : \mathbb{R}^n \rightarrow \mathbb{R}^{1 \times n}$ is defined by $q'(x) \triangleq \frac{\partial q(x)}{\partial x}$. The Lie derivative of q along the vector fields of $v : \mathbb{R}^n \rightarrow \mathbb{R}^{n \times 1}$ is defined as $L_v q(x) \triangleq q'(x)v(x)$. If $l = 1$, then for all positive integers r , define $L_v^r q(x) \triangleq L_v L_v^{r-1} q(x)$. In this paper, we assume that all functions are sufficiently smooth such that all derivatives that we write exist and are continuous.

The boundary of $B \subseteq \mathbb{R}^n$ is denoted by $\text{bd } B$. Let $\|\cdot\|$ denote the 2 norm on \mathbb{R}^n . The maximum eigenvalue of $A \in \mathbb{R}^{n \times n}$ is denoted by $\lambda_{\max}(A)$.

III. PROBLEM FORMULATION

Consider the dynamic system

$$\dot{x}(t) = f(x(t)) + \phi(x(t))\theta_* + g(x(t))u(t), \quad (1)$$

where $x(t) \in \mathbb{R}^n$ is the state; $x(0) = x_0 \in \mathbb{R}^n$ is the initial condition; $u : [0, \infty) \rightarrow \mathbb{R}^m$ is the control; $f : \mathbb{R}^n \rightarrow \mathbb{R}^n$, $g : \mathbb{R}^n \rightarrow \mathbb{R}^{n \times m}$, and $\phi : \mathbb{R}^n \rightarrow \mathbb{R}^{n \times p}$ are locally Lipschitz continuous on \mathbb{R}^n ; $\theta_* \in \Theta$ is an unknown parameter; and $\Theta \subset \mathbb{R}^p$ is assumed to be bounded and known.

Let $\psi_0 : \mathbb{R}^n \rightarrow \mathbb{R}$ be continuously differentiable, and define the *safe set*

$$C_0 \triangleq \{x \mid \psi_0(x) \geq 0\}, \quad (2)$$

which is the set of states that satisfy the state constraint. We make the following assumption:

Assumption 1. There exists a positive integer d such that for all $i \in \{0, 1, \dots, d-2\}$ and all $x \in \mathbb{R}^n$, $L_g L_f^i \psi_0(x) = 0$ and $L_\phi L_f^i \psi_0(x) = 0$.

Assumption 1 implies that the relative degree of ψ_0 with respect to the control u and the unknown parameter θ_* is at least d on \mathbb{R}^n . Thus, we use a higher-order approach to construct a candidate CBF. For all $i \in \{1, \dots, d-1\}$, let $\alpha_{i-1} : \mathbb{R} \rightarrow \mathbb{R}$ is a $(d-i)$ -times continuously differentiable extended class- \mathcal{K} function, and define

$$\psi_i(x) \triangleq L_f \psi_{i-1}(x) + \alpha_{i-1}(\psi_{i-1}(x)). \quad (3)$$

For all $i \in \{1, \dots, d-1\}$, the zero-superlevel set of ψ_i is given by

$$C_i \triangleq \{x \mid \psi_i(x) \geq 0\}. \quad (4)$$

We make the following assumption:

Assumption 2. For all $x \in \text{bd } C_{d-1}$, $L_g L_f^{d-1} \psi_0(x) \neq 0$.

Assumption 2 implies that ψ_0 has relative degree d with respect to the control u on $\text{bd } C_{d-1}$. Thus,

$$\bar{C} \triangleq \bigcap_{i=0}^{d-1} C_i \quad (5)$$

is control forward invariant.

Next, consider the desired control $u_d : \mathbb{R}^n \times \mathbb{R}^p \rightarrow \mathbb{R}^m$, which is designed to satisfy performance requirements but may not satisfy the state constraint that $x(t) \in C_0$ for all t . The desired control $u_d(x, \hat{\theta})$ is a function of the state x and can be parameterized $\hat{\theta}$, which represents an estimate of the unknown parameter θ_* . In other words, $u_d(x, \theta_*)$ is the ideal desired control.

Consider the cost function $J : \mathbb{R}^n \times \mathbb{R}^p \times \mathbb{R}^m \rightarrow \mathbb{R}$ defined by

$$J(x, \hat{\theta}, \hat{u}) \triangleq \frac{1}{2} \left(\hat{u} - u_d(x, \hat{\theta}) \right)^T H(x, \hat{\theta}) \left(\hat{u} - u_d(x, \hat{\theta}) \right), \quad (6)$$

where $H : \mathbb{R}^n \times \mathbb{R}^p \rightarrow \mathbb{R}^{m \times m}$ is locally Lipschitz, and for all $(x, \hat{\theta}) \in \mathbb{R}^n \times \mathbb{R}^p$, $H(x, \hat{\theta})$ is positive definite.

The objective is twofold. First, design a feedback control that for all $(x, \hat{\theta})$, minimizes (6) subject to the state constraint that $x(t) \in \bar{C}$ for all $t \geq 0$. Second, we aim to estimate θ_* so that the desired control $u_d(x, \hat{\theta})$ approaches the ideal desired control $u_d(x, \theta_*)$.

IV. PARAMETER ESTIMATION

This section provides a method of estimating θ_* , and provides a computable upper bound on the norm of the parameter estimation error. This computable upper bound is nonincreasing and used in subsequent sections to design a safe control that is not overly conservative.

Unless otherwise stated, all expressions with subscript k are for all $k \in \mathbb{N} \triangleq \{0, 1, 2, 3, \dots\}$. Let $t_0 = 0$, and let $t_{k+1} > t_k$. Define

$$\Phi_k \triangleq \int_{t_k}^{t_{k+1}} \phi(x(t)) dt, \quad (7)$$

and for all negative integers i , let $\Phi_i = 0_{n \times p}$. Next, let k_n be a nonnegative integer, and define

$$P_k \triangleq (\sigma_k I_p + \Omega_k)^{-1} \in \mathbb{R}^{p \times p}, \quad (8)$$

where $\sigma_k > 0$ and

$$\Omega_k \triangleq \sum_{i=k-k_n}^k \Phi_i^T \Phi_i. \quad (9)$$

Define

$$y_k \triangleq x(t_{k+1}) - x(t_k) - \int_{t_k}^{t_{k+1}} f(x(t)) + g(x(t))u(t) dt. \quad (10)$$

The next result shows that y_k is a linear regression in Φ_k and the unknown parameter θ_* .

Proposition 1. For all $k \in \mathbb{N}$, $y_k = \Phi_k \theta_*$.

Proof. It follows from (1) that

$$\dot{x}(t) \theta_* = \dot{x}(t) - f(x(t)) - g(x(t))u(t),$$

and integrating over $[t_k, t_{k+1})$ yields

$$\begin{aligned} \Phi_k \theta_* &= x(t_{k+1}) - x(t_k) \\ &\quad - \int_{t_k}^{t_{k+1}} f(x(t)) + g(x(t))u(t) dt. \end{aligned}$$

Then, (10) implies that $y_k = \Phi_k \theta_*$. \square

Next, consider the regularized finite-horizon least-squares cost $\mathcal{J}_k : \mathbb{R}^p \rightarrow \mathbb{R}$ defined by

$$\mathcal{J}_k(\hat{\theta}) \triangleq \sigma_k \|\hat{\theta} - \theta_k\|^2 + \sum_{i=k-k_n}^k \|\Phi_i \hat{\theta} - y_i\|^2.$$

For all $k \in \mathbb{N}$, the minimizer of \mathcal{J}_k is given by

$$\theta_{k+1} \triangleq P_k \left(\sum_{i=k-k_n}^k \Phi_i^T y_i + \sigma_k \theta_k \right), \quad (11)$$

where $\theta_0 \in \mathbb{R}^p$. The finite-horizon least-squares estimator (11) can also be expressed in recursive form. See [32] for details.

Next, define

$$\tilde{\theta}_k \triangleq \theta_k - \theta_*, \quad (12)$$

and consider the Lyapunov-like function

$$V_k \triangleq \tilde{\theta}_k^T \tilde{\theta}_k, \quad (13)$$

and the Lyapunov-like difference

$$\Delta V_k \triangleq \tilde{\theta}_{k+1}^T \tilde{\theta}_{k+1} - \tilde{\theta}_k^T \tilde{\theta}_k. \quad (14)$$

The next result provides properties of the finite-horizon least-squares estimator (7)–(11).

Proposition 2. The following statements holds:

- (a) For all $k \in \mathbb{N}$, $\Delta V_k = -\tilde{\theta}_k^T (I_p - \sigma_k^2 P_k^2) \tilde{\theta}_k \leq 0$.
- (b) $\{\theta_k\}_{k=0}^\infty$ is bounded.
- (c) Assume there exists $k_i \in \mathbb{N}$ such that for all $k \geq k_i$, Ω_k is full rank. Then, $\theta_k \rightarrow \theta_*$ as $k \rightarrow \infty$.

Proof. Note that it follows from (11) that

$$\tilde{\theta}_{k+1} = \tilde{\theta}_k - P_k \Omega_k \tilde{\theta}_k. \quad (15)$$

Since (8) implies that $\Omega_k = P_k^{-1} - \sigma_k I_p$, it follows from (15) that

$$\tilde{\theta}_{k+1} = \sigma_k P_k \tilde{\theta}_k. \quad (16)$$

Evaluating the Lyapunov-like difference (14) along (16) yields

$$\begin{aligned} \Delta V_k &= -\tilde{\theta}_k^T (I_p - \sigma_k^2 P_k^2) \tilde{\theta}_k \\ &\leq \left(\sigma_k^2 \lambda_{\max}(P_k)^2 - 1 \right) \|\tilde{\theta}_k\|^2, \end{aligned} \quad (17)$$

and it follow from (8) that $\sigma_k^2 \lambda_{\max}(P_k)^2 - 1 \leq 0$, which confirms (a).

To prove (b), since $\Delta V_k \leq 0$, it follows that $\tilde{\theta}_k$ is bounded. Since, in addition, $\tilde{\theta}_k = \theta_k - \theta_*$, it follows that θ_k is bounded.

To prove (c), since Ω_k is full rank, it follows from (8) that $\sigma_k^2 \lambda_{\max}(P_k)^2 - 1 < 0$, which combined with (17) implies that $\Delta V_k < 0$ for all $\tilde{\theta}_k \neq 0$. Thus, $\tilde{\theta}_k \rightarrow 0$ as $k \rightarrow \infty$, which confirms (c). \square

Define

$$\bar{y}_i(\theta_k) \triangleq \Phi_i \theta_k - y_i, \quad (18)$$

and define

$$\begin{aligned} \tau_k &\triangleq \frac{2}{\sigma_k} \left[- \sum_{i=k-k_n}^k \|\bar{y}_i(\theta_k)\|^2 \right. \\ &\quad \left. + \left(\sum_{i=k-k_n}^k \bar{y}_i^T(\theta_k) \Phi_i \right) P_k \left(\sum_{i=k-k_n}^k \Phi_i^T \bar{y}_i(\theta_k) \right) \right] \\ &\quad + \left(\sum_{i=k-k_n}^k \bar{y}_i^T(\theta_k) \Phi_i \right) P_k^2 \left(\sum_{i=k-k_n}^k \Phi_i^T \bar{y}_i(\theta_k) \right), \end{aligned} \quad (19)$$

The next result shows that the computable quantity τ_k is equal to the Lyapunov-like difference ΔV_k , which cannot be computed from its definition because θ_* is unknown.

Lemma 1. For all $k \in \mathbb{N}$, $\tau_k = \Delta V_k$.

Proof. Proposition 1 and (18) imply $\bar{y}_i(\theta_k) = \Phi_i \tilde{\theta}_k$, and substituting into (19) yields

$$\tau_k = \frac{2}{\sigma_k} \tilde{\theta}_k^T (-\Omega_k + \Omega_k P_k \Omega_k) \tilde{\theta}_k + \tilde{\theta}_k^T \Omega_k P_k^2 \Omega_k \tilde{\theta}_k.$$

Since (8) implies that $\Omega_k = P_k^{-1} - \sigma_k I_p$, it follows that $\tau_k = \tilde{\theta}_k^T (-I_p + \sigma_k^2 P_k^2) \tilde{\theta}_k$, which combined with (a) of Proposition 2 yields $\tau_k = \Delta V_k$. \square

Next, let $\nu_0 > 0$ satisfy

$$\nu_0 \geq \sup_{\tilde{\theta} \in \Theta} \|\theta_0 - \tilde{\theta}\|, \quad (20)$$

and note that ν_0 satisfying (20) can be computed because the set Θ is known. For all $k \in \mathbb{N}$, define

$$\nu_{k+1} \triangleq \min \left(\sigma_k \lambda_{\max}(P_k) \nu_k, \sqrt{\nu_k^2 + \tau_k} \right), \quad (21)$$

and the following result shows that ν_k is a nonincreasing upper bound on the magnitude of the estimation error $\tilde{\theta}_k$.

Proposition 3. The following statements holds:

- (a) For all $k \in \mathbb{N}$, $\nu_k \geq \|\tilde{\theta}_k\|$.
- (b) For all $k \in \mathbb{N}$, $\nu_{k+1} \leq \nu_k$.
- (c) $\{\nu_k\}_{k=0}^\infty$ is bounded.
- (d) Assume there exists $k_i \in \mathbb{N}$ such that for all $k \geq k_i$, Ω_k is full rank. Then, $\nu_k \rightarrow 0$ as $k \rightarrow \infty$.

Proof. To prove (a), it follows from (14) and (a) of Proposition 2 that

$$\|\tilde{\theta}_{k+1}\| \leq \sigma_k \lambda_{\max}(P_k) \|\tilde{\theta}_k\|. \quad (22)$$

We use induction on k . First, since $\theta_* \in \Theta$, it follows from (20) that $\nu_0 \geq \|\tilde{\theta}_0\|$, which proves (a) for $k = 0$. Next, let $j \in \mathbb{N}$, and assume for induction that $\nu_j \geq \|\tilde{\theta}_j\|$. Thus, (21) implies that

$$\nu_{j+1} \geq \min \left(\sigma_j \lambda_{\max}(P_j) \|\tilde{\theta}_j\|, \sqrt{\|\tilde{\theta}_j\|^2 + \tau_j} \right),$$

which combined with (22) yields

$$\nu_{j+1} \geq \min \left(\|\tilde{\theta}_{j+1}\|, \sqrt{\|\tilde{\theta}_j\|^2 + \tau_j} \right). \quad (23)$$

Since Lemma 1 and (14) imply that $\sqrt{\|\tilde{\theta}_k\|^2 + \tau_k} = \|\tilde{\theta}_{k+1}\|$, it follows from (23) that $\nu_{j+1} \geq \|\tilde{\theta}_{j+1}\|$, which confirms (a).

To prove (b), it follows from Lemma 1 and (a) of Proposition 2 that $\sqrt{\nu_k^2 + \tau_k} \leq \nu_k$, which combined with (21) confirms (b).

To prove (c), since (21) implies that ν_k is nonnegative, it follows from (b) that $\{\nu_k\}_{k=0}^\infty$ is bounded, which confirms (c).

To prove (d), note that, since Ω_k is full rank, it follows that $\lambda_{\max}(\sigma_k P_k) < 1$ and $\tau_k \leq 0$, which implies that $\lambda_{\max}(\sigma_k P_k) \nu_k < \nu_k$ and $\sqrt{\nu_k^2 + \tau_k} \leq \nu_k$ and consequently from (21), $\nu_{k+1} < \nu_k$. From (a), note that $\|\tilde{\theta}_{k+1}\| \leq \nu_{k+1} < \nu_k$. Finally, since $\|\tilde{\theta}_{k+1}\| \rightarrow 0$ as $k \rightarrow \infty$, it follows that $\nu_k \rightarrow 0$ as $k \rightarrow \infty$. \square

The next section uses the estimate θ_k and the computable upper bound ν_k to develop a safe an optimal control.

V. SAFE AND OPTIMAL CONTROL

Let $\xi : [0, \infty) \rightarrow [0, 1]$ be a nondecreasing and continuously differentiable function such that for all $t \in (-\infty, 0]$,

$\xi(t) = 0$ and for all $t \in [1, \infty)$, $\xi(t) = 1$. The following example provides one possible choice for ξ .

Example 1. Let $\eta \geq 1$, and consider

$$\xi(t) \triangleq \begin{cases} 0, & t \in (-\infty, 0), \\ \eta t - \frac{\sin 2\pi\eta t}{2\pi}, & t \in [0, \frac{1}{\eta}], \\ 1, & t \in (\frac{1}{\eta}, \infty). \end{cases} \quad (24)$$

Figure 1 shows (24) for $\eta \in \{1, 2, 5\}$. \triangle

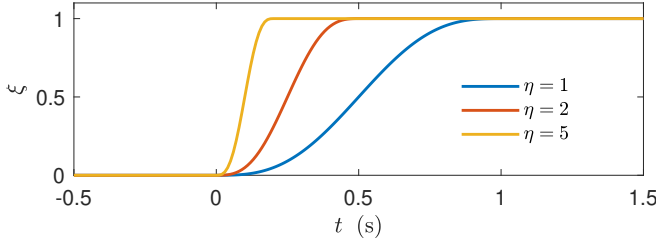


Fig. 1: ξ given by Example 1.

Define $\mathcal{T}_k \triangleq [t_k, t_{k+1})$. For all $k \in \mathbb{N}$ and all $t \in \mathcal{T}_k$, let $\theta : \mathcal{T}_k \rightarrow \mathbb{R}^p$ be given by

$$\theta(t) \triangleq \xi \left(\frac{t - t_k}{t_{k+1} - t_k} \right) \theta_k + \left[1 - \xi \left(\frac{t - t_k}{t_{k+1} - t_k} \right) \right] \theta_{k-1}, \quad (25)$$

and let $\nu : \mathcal{T}_k \rightarrow [0, \infty)$ be given by

$$\nu(t) \triangleq \xi \left(\frac{t - t_k}{t_{k+1} - t_k} \right) \nu_k + \left[1 - \xi \left(\frac{t - t_k}{t_{k+1} - t_k} \right) \right] \nu_{k-1}, \quad (26)$$

where $\nu_{-1} \triangleq \nu_0$ and $\theta_{-1} \triangleq \theta_0$. Note that ν and θ are continuously differentiable functions constructed from the sequences ν_k and θ_k .

Next, let $\alpha : \mathbb{R} \rightarrow \mathbb{R}$ be locally Lipschitz and nondecreasing such that $\alpha(0) = 0$, and consider the state-constraint function $\psi : \mathbb{R}^n \times \mathbb{R}^p \times \mathbb{R} \times \mathbb{R}^m \times \mathbb{R} \rightarrow \mathbb{R}$ be defined by

$$\begin{aligned} \psi(x, \hat{\theta}, \hat{\nu}, \hat{u}, \hat{\delta}) \triangleq & L_f \psi_{d-1}(x) + L_g \psi_{d-1}(x) \hat{\nu} \\ & + L_\phi \psi_{d-1}(x) \hat{\theta} - \|L_\phi \psi_{d-1}(x)\| \hat{\nu} \\ & + \alpha_{d-1}(\psi_{d-1}(x)) + \hat{\delta} \psi_{d-1}(x), \end{aligned} \quad (27)$$

where \hat{u} is the control variable and $\hat{\delta}$ is a slack variable. Define

$$\psi_*(x, \hat{u}, \hat{\delta}) \triangleq \psi(x, \theta_*, 0, \hat{u}, \hat{\delta}), \quad (28)$$

and note that $\psi_*(x(t), \hat{u}, \hat{\delta}) \geq 0$ is a CBF-based state constraint for (1) that guarantees for all $t \geq 0$, $x(t) \in \bar{C}$. However, ψ_* depends on the unknown parameter θ_* . The next result shows that if $\hat{\nu} \geq \|\hat{\theta} - \theta_*\|$, then ψ is a lower bound for ψ_* . Since (a) of Proposition 3 implies that $\nu(t) \geq \|\theta(t) - \theta_*\|$, the next result also demonstrates that the estimate θ and upper bound ν can be used in (27) to obtain a constraint that is sufficient for $\psi_*(x(t), \hat{u}, \hat{\delta}) \geq 0$.

Proposition 4. Let $x \in \mathbb{R}^n$, $\hat{u} \in \mathbb{R}^m$, and $\hat{\delta} \in \mathbb{R}$. Then, the following hold:

(a) Let $\hat{\theta} \in \mathbb{R}^p$ and let $\hat{\nu} \geq \|\hat{\theta} - \theta_*\|$. Then, $\psi(x, \hat{\theta}, \hat{\nu}, \hat{u}, \hat{\delta}) \leq \psi_*(x, \hat{u}, \hat{\delta})$.

(b) For all $t \geq 0$, $\psi(x, \theta(t), \nu(t), \hat{u}, \hat{\delta}) \leq \psi_*(x, \hat{u}, \hat{\delta})$.

(c) Assume there exists $k_i \in \mathbb{N}$ such that for all $k \geq k_i$, Ω_k is full rank. Then, $\lim_{t \rightarrow \infty} \psi(x, \theta(t), \nu(t), \hat{u}, \hat{\delta}) = \psi_*(x, \hat{u}, \hat{\delta})$

Proof. To prove (a), since $\hat{\nu} \geq \|\hat{\theta} - \theta_*\|$, it follows that

$$L_\phi \psi_{d-1}(x) [\hat{\theta} - \theta_*] \leq \|L_\phi \psi_{d-1}(x)\| \|\hat{\theta} - \theta_*\| \leq \|L_\phi \psi_{d-1}(x)\| \hat{\nu},$$

which implies

$$L_\phi \psi_{d-1}(x) \theta_* \geq L_\phi \psi_{d-1}(x) \hat{\theta} - \|L_\phi \psi_{d-1}(x)\| \hat{\nu}.$$

Adding $L_f \psi_{d-1}(x) + L_g \psi_{d-1}(x) \hat{u} + \hat{\delta} \psi_{d-1}(x) + \alpha_{d-1}(\psi_{d-1}(x))$ to both sides yields $\psi_*(x, \hat{u}, \hat{\delta}) \geq \psi(x, \hat{\theta}, \hat{\nu}, \hat{u}, \hat{\delta})$.

To prove (b), it follows from (25) that

$$\|\theta(t) - \theta_*\| \leq \xi \|\theta_k - \theta_*\| + (1 - \xi) \|\theta_{k-1} - \theta_*\|, \quad (29)$$

where the argument of ξ is omitted for brevity. Next, using (a) of Proposition 3 and (26) yields

$$\|\theta(t) - \theta_*\| \leq \xi \nu_k + (1 - \xi) \nu_{k-1} = \nu(t).$$

Since $\nu(t) \geq \|\theta(t) - \theta_*\|$, it follows from (a) that $\psi_*(x, \hat{u}, \hat{\delta}) \geq \psi(x, \theta(t), \nu(t), \hat{u}, \hat{\delta})$.

To prove (c), note that (25) and (c) of Proposition 2 imply that $\lim_{t \rightarrow \infty} \theta(t) = \theta_*$. Similarly, (26) and (d) of Proposition 3 imply that $\lim_{t \rightarrow \infty} \nu(t) = 0$. Thus, it follows from (27) and (28) that $\lim_{t \rightarrow \infty} \psi(x, \theta(t), \nu(t), \hat{u}, \hat{\delta}) = \psi_*(x, \hat{u}, \hat{\delta})$. \square

Next, let $\beta > 0$, and consider the cost function $\bar{J} : \mathbb{R}^n \times \mathbb{R}^p \times \mathbb{R}^m \times \mathbb{R} \rightarrow \mathbb{R}$ given by

$$\bar{J}(x, \theta, \hat{u}, \hat{\delta}) = J(x, \theta, \hat{u}) + \frac{\beta}{2} \hat{\delta}^2, \quad (30)$$

which is equal to (6) plus a term that weights the slack variable $\hat{\nu}$. For each $t \geq 0$, the objective is to synthesize $(\hat{u}, \hat{\delta})$ that minimizes $\bar{J}(x(t), \theta(t), \hat{u}, \hat{\delta})$ subject to the CBF state constraint $\psi(x(t), \theta(t), \nu(t), \hat{u}, \hat{\delta}) \geq 0$.

For all $(x, \theta, \nu) \in \mathbb{R}^n \times \mathbb{R}^p \times \mathbb{R}$, the minimizer of $\bar{J}(x, \theta, \hat{u}, \hat{\delta})$ subject to $\psi(x, \theta, \nu, \hat{u}, \hat{\delta})$ can be obtained from the first-order necessary conditions for optimality. For example, see [10], [11], [23], [24], [33]. The first-order necessary conditions yield the control $u_* : \mathbb{R}^n \times \mathbb{R}^p \times \mathbb{R} \rightarrow \mathbb{R}^m$ defined by

$$u_*(x, \theta, \nu) \triangleq u_d(x, \theta) + \lambda_*(x, \theta, \nu) H(x, \theta)^{-1} L_g \psi_{d-1}(x)^T, \quad (31)$$

and the slack variable $\delta_* : \mathbb{R}^n \times \mathbb{R}^p \times \mathbb{R} \rightarrow \mathbb{R}$ given by

$$\delta_*(x, \theta, \nu) \triangleq \beta^{-1} \psi_{d-1}(x) \lambda_*(x, \theta, \nu), \quad (32)$$

where $\lambda_* : \mathbb{R}^n \times \mathbb{R}^p \times \mathbb{R} \rightarrow \mathbb{R}$ is defined by

$$\lambda_*(x, \theta, \nu) \triangleq \begin{cases} -\frac{\omega(x, \theta, \nu)}{q(x, \theta)}, & \omega(x, \theta, \nu) < 0, \\ 0, & \omega(x, \theta, \nu) \geq 0, \end{cases} \quad (33)$$

and $q : \mathbb{R}^n \times \mathbb{R}^p \rightarrow \mathbb{R}$ and $\omega : \mathbb{R}^n \times \mathbb{R}^p \times \mathbb{R} \rightarrow \mathbb{R}$ are given

by

$$q(x, \theta) \triangleq L_g \psi_{d-1}(x) H(x, \theta)^{-1} L_g \psi_{d-1}(x)^T + \beta^{-1} \psi_{d-1}(x)^2, \quad (34)$$

$$\omega(x, \theta, \nu) \triangleq \psi(x, \theta, \nu, u_d(x, \theta), 0). \quad (35)$$

The next result shows that $(u_*(x, \theta, \nu), \delta_*(x, \theta, \nu))$ is the unique global minimizer of $\bar{J}(x, \theta, \hat{u}, \hat{\delta})$ subject to $\psi(x, \theta, \nu, \hat{u}, \hat{\delta})$. The proof is similar to that of [24, Theorem 1] and is omitted for space.

Theorem 1. Assume Assumption 2 is satisfied. Let $(x, \theta, \nu) \in \mathbb{R}^n \times \mathbb{R}^p \times \mathbb{R}$, and let $(\hat{u}, \hat{\delta}) \in \mathbb{R}^m \times \mathbb{R}$ be such that $(\hat{u}, \hat{\delta}) \neq (u_*(x, \theta, \nu), \delta_*(x, \theta, \nu))$ and $\psi(x, \theta, \nu, \hat{u}, \hat{\delta}) \geq 0$. Then,

$$\bar{J}(x, \theta, \hat{u}, \hat{\delta}) > \bar{J}(x, \theta, u_*(x, \theta, \nu), \delta_*(x, \theta, \nu)).$$

The following theorem is the main result on satisfaction of the state constraint despite the model uncertainty. This result follows from standard CBF analysis techniques (e.g., [11]) and is omitted for space.

Theorem 2. Consider (1), where Assumptions 1 and 2 are satisfied. Let $u = u_*$, where u_* is given by (31)–(35), where θ and ν are given by (7)–(11), (18), (19), (21), (25), and (26). Assume that ψ'_{d-1} is locally Lipschitz. Then, for all $x_0 \in \bar{\mathcal{C}}$, the following statements hold:

- (a) There exists a maximum value $t_m(x_0) \in (0, \infty]$ such that (1) with $u = u_*$ has a unique solution on $[0, t(x_0))$.
- (b) For all $t \in [0, t(x_0))$, $x(t) \in \bar{\mathcal{C}}$.
- (c) Assume the maximum interval of existence and uniqueness is $t(x_0) = \infty$. Then, for all $t \geq 0$, $x(t) \in \bar{\mathcal{C}}$.

Theorems 1 and 2 demonstrate that the control (31)–(35) satisfies the state constraint that for all $t \geq 0$, $x(t) \in \mathcal{C}_0$, and yields a control that is optimal with respect to a constraint optimization that aims to obtain a control as close as possible to u_d subject to the state constraint.

VI. INVERTED PENDULUM

Consider the pendulum modeled by (1), where

$$f(x) = \begin{bmatrix} \dot{\gamma} \\ f_2(x) \end{bmatrix}, \quad g(x) = \begin{bmatrix} 0 \\ \frac{1}{mL^2} \end{bmatrix}, \quad \phi(x) = \begin{bmatrix} 0 \\ \phi_2(x) \end{bmatrix},$$

where

$$\phi_2(x) \triangleq \frac{1}{mL^2} \begin{bmatrix} -\gamma & -\gamma^3 & -\tanh \frac{\dot{\gamma}}{\epsilon_1} & -\dot{\gamma} & -\dot{\gamma}^2 \tanh \frac{\dot{\gamma}}{\epsilon_2} \end{bmatrix},$$

$$f_2(x) \triangleq \frac{g}{L} \sin \gamma, \quad x = \begin{bmatrix} \gamma \\ \dot{\gamma} \end{bmatrix},$$

and γ is the position, $\dot{\gamma}$ is the velocity, g is the gravity, $\epsilon_1 = \epsilon_2 = 2$, $m = 0.01$ kg and $L = 0.15$ m. In $\phi_2(x)$ the first two entries represent linear and cubic restitution forces, while the last three entries represent coulomb friction, viscous friction and drag force. Furthermore, $\theta_* = [0.5 \ 0.35 \ 0.15 \ 0.5 \ 0.25]^T \in \Theta$, where

$$\Theta = \left\{ \hat{\theta} \in \mathbb{R}^5 \mid \text{for all } j \in \{1, 2, \dots, 5\}, e_j^T \hat{\theta} \in [0, 2.5] \right\}, \quad (36)$$

and e_j is the j th column of the $p \times p$ identity matrix.

We implement (7)–(11), (18), (19), (21), (25), and (26), where $t_{k+1} - t_k = 0.25$ s, $k_n = 30$, $\theta_0 = 0$, $\nu_0 = \sup_{\hat{\theta} \in \Theta} \|\theta_0 - \hat{\theta}\|$, $\sigma_k = 0.1$ and $\eta = 2$.

Let $\gamma_d(t) \triangleq -0.99(\pi/4) \cos t$ be the desired angular position. Define the error $e \triangleq \gamma - \gamma_d$ and the desired control

$$u_d(\hat{\theta}) \triangleq mL^2 \left[-f_2 - \phi_2 \hat{\theta} + \dot{\omega}_d - K_1 e - K_2 \dot{e} \right],$$

where $K_1 = 50$ and $K_2 = 100$.

If $u(t) = u_d(\theta_*)$, then $\ddot{e} + K_1 \dot{e} + K_2 e = 0$, which implies that $\lim_{t \rightarrow \infty} e(t) = 0$ and $\lim_{t \rightarrow \infty} \dot{e}(t) = 0$.

The safe set is given by (2), where $d = 2$ and

$$\psi_0(x) = \left(\frac{\pi}{4} \right)^2 - \gamma^2. \quad (37)$$

We implement the control (31)–(35), where $H = 2$, $\beta = 200$ and $\alpha_0 = \alpha_1 = 200$. The control is updated at 1000 Hz using a zero-order hold.

To examine the impact of the adaptive estimate θ and the adaptive bound ν , we consider 3 cases:

- a) Adaptive estimate θ and adaptive bound ν are used in CBF constraint and desired control (i.e., $\psi = \psi(x, \theta, \nu, \hat{u}, \hat{\delta})$, $u_d = u_d(\theta)$).
- b) Adaptive estimate θ and adaptive bound ν are used in CBF constraint (i.e., $\psi = \psi(x, \theta, \nu, \hat{u}, \hat{\delta})$), but the desired control uses initial estimate (i.e., $u_d = u_d(\theta_0)$).
- c) Initial estimate θ_0 and initial bound ν_0 are used in CBF constraint (i.e., $\psi = \psi(x, \theta_0, \nu_0, \hat{u}, \hat{\delta})$), but the desired control uses the adaptive estimate (i.e., $u_d = u_d(\theta)$).

Proposition 4 implies that all 3 cases satisfy the state constraint. However, Cases 2 and 3 use the initial estimates, which can be conservative and may lead to worse performance, that is, worse tracking of γ_d .

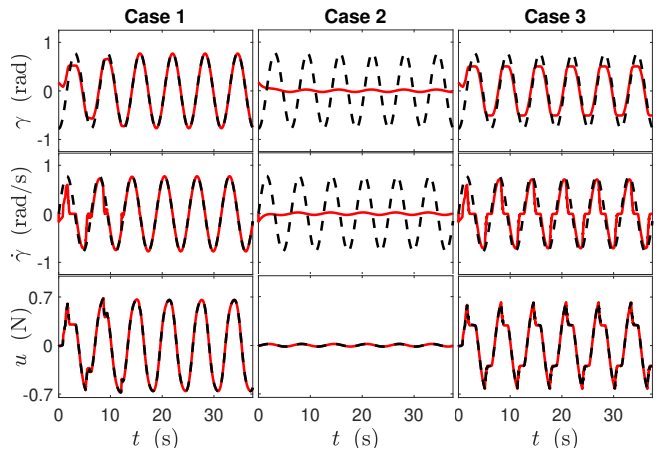


Fig. 2: γ , $\dot{\gamma}$ and u for Cases 1, 2 and 3. Note that γ_d , $\dot{\gamma}_d$ and u_d are shown with dashed lines.

Figure 2 shows γ , $\dot{\gamma}$ and u , where $x(0) = [0.1745 \ 0]^T$. In Case 1 it is shown that $\lim_{t \rightarrow \infty} \gamma(t) = \gamma_d$ and $\lim_{t \rightarrow \infty} \dot{\gamma}(t) = \dot{\gamma}_d$, unlike in Case 2. In Case 3, γ and $\dot{\gamma}$ diverges from γ_d and $\dot{\gamma}_d$ near to $\gamma = \pm \frac{\pi}{4}$ rad.

Figure 3 shows that, for all $t \geq 0$, ψ_0 , ψ_1 and ψ remain nonnegative in all cases. In Case 1, the safety constraint is

not active in steady-state. In Case 2, for all $t \geq 0$, $\psi(x(t)) > 0$. Finally, in Case 3, the safety constraint is periodically activated due to its inherent conservativeness, explaining why γ and $\dot{\gamma}$ diverge from γ_d and ω_d near to $\gamma = \pm \frac{\pi}{4}$ rad.

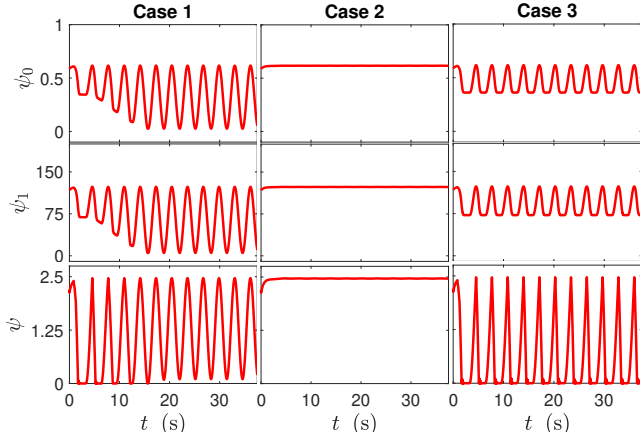


Fig. 3: ψ_0 , ψ_1 and ψ for Cases 1, 2 and 3.

Figures 4 and 5 show that for Cases 1 and 3, $\lim_{t \rightarrow \infty} \theta(t) = \theta_*$ and $\lim_{t \rightarrow \infty} \nu(t) = 0$, unlike in Case 2.

VII. NONHOLONOMIC MOBILE ROBOT

Consider the nonholonomic differential drive mobile robot modeled by (1), where

$$f(x) = \begin{bmatrix} v \cos \gamma - l_d \omega \sin \gamma \\ v \sin \gamma + l_d \omega \cos \gamma \\ \omega \\ 0 \\ 0 \end{bmatrix}, \quad g(x) = \begin{bmatrix} 0 & 0 \\ 0 & 0 \\ 0 & 0 \\ g_1(x) & g_2(x) \end{bmatrix},$$

$$\phi(x) = \begin{bmatrix} 0 \\ 0 \\ 0 \\ \phi_4(x) \\ \phi_5(x) \end{bmatrix}, \quad x = \begin{bmatrix} q_x \\ q_y \\ \gamma \\ v \\ \omega \end{bmatrix}, \quad u = \begin{bmatrix} u_r \\ u_l \end{bmatrix}, \quad \theta_* = \begin{bmatrix} k_{b1} \\ k_{b2} \\ \epsilon \\ \kappa \end{bmatrix},$$

where

$$\phi_4(x) \triangleq \begin{bmatrix} -\frac{k_m \omega_r}{mrR_a} & -\frac{k_m \omega_l}{mrR_a} & -\frac{\omega_r}{mr} & -\frac{\omega_l}{mr} & -g \sin \gamma \end{bmatrix},$$

$$\phi_5(x) \triangleq \begin{bmatrix} -\frac{k_m l \omega_r}{IrR_a} & \frac{k_m l \omega_l}{IrR_a} & -\frac{\omega_r l}{Ir} + \frac{\omega_l l}{Ir} & 0 \end{bmatrix},$$

$$g_1(x) \triangleq \begin{bmatrix} \frac{k_m}{mrR_a} & \frac{k_m l}{IrR_a} \end{bmatrix}^T, \quad g_2(x) \triangleq \begin{bmatrix} \frac{k_m}{mrR_a} & -\frac{k_m l}{IrR_a} \end{bmatrix}^T,$$

$$\omega_r \triangleq \frac{2v + l\omega}{2r}, \quad \omega_l \triangleq \frac{2v - l\omega}{2r},$$

and $[q_x \ q_y]^T$ denote the position of the tip of the robot in an orthogonal coordinate frame, γ is the direction of the velocity vector, v and ω are the velocity and angular velocity, u_r and u_l are the voltage of each motor, $k_m = 0.1$ N.m/Amp is the torque constant, $r = 0.1$ m is the wheel radius, $l = 0.5$ m is the distance between wheels, $l_d = 0.25$ m is the distance

from the center of mass to the tip of the vehicle, $R_a = 0.27$ ohms is the armature resistance, $m = 10$ kg and $I = 0.83$ kg.m² are the vehicle mass and inertia, ω_r and ω_l are the angular velocity of the each wheel and g is the gravity [34]. Moreover, $k_{b1} = k_{b2} = 0.0487$ V/(rad/sec) are the back-EMF constants of each motor, $\epsilon = 0.025$ is a friction coefficient, and $\kappa = 0.5$ corresponds to an angle of inclination of the ground of 30° .

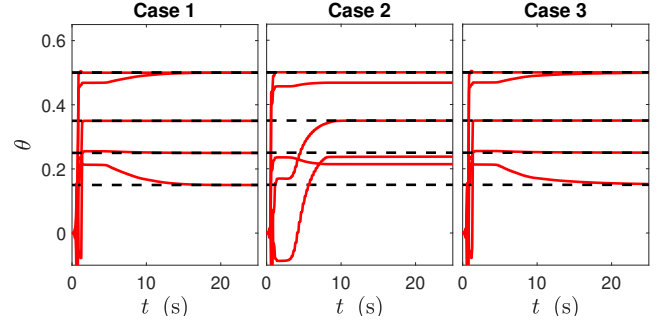


Fig. 4: θ for Cases 1, 2 and 3. Note that θ_* is shown using dashed line.

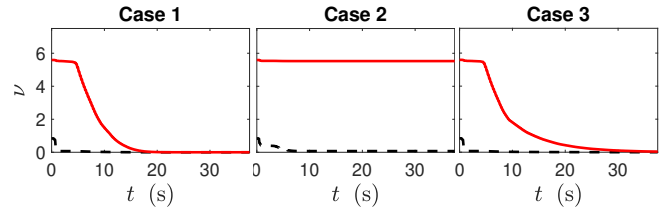


Fig. 5: ν for Cases 1, 2 and 3. Note that $\|\tilde{\theta}_k\|$ is shown with dashed line.

Let θ_* be in the set

$$\Theta = \left\{ \hat{\theta} \in \mathbb{R}^4 \mid e_1^T \hat{\theta} \in [0, 5], e_2^T \hat{\theta} \in [0, 5], e_3^T \hat{\theta} \in [0, 5], e_4^T \hat{\theta} \in [0, 1] \right\}.$$

We implement (7)–(11), (18), (19), (21), (25), and (26), where $t_{k+1} - t_k = 0.1$ s, $k_n = 10$, $\theta_0 = [0.1 \ 0.1 \ 0.1 \ 0.1]^T$, $\nu_0 = \sup_{\hat{\theta} \in \Theta} \|\theta_0 - \hat{\theta}\|$, $\sigma_k = 0.001$ and $\eta = 2$.

The desired linear and angular velocity [22] are

$$v_d \triangleq -(\mu_1 + \mu_2)v - (1 + \mu_1 \mu_2)e_1 + \frac{\mu_1^2}{l_d} e_2^2, \quad \omega_d \triangleq -\frac{\mu_1}{l_d} e_2,$$

where

$$e_1 \triangleq (q_x - q_{dx}) \cos \gamma + (q_y - q_{dy}) \sin \gamma,$$

$$e_2 \triangleq -(q_x - q_{dx}) \sin \gamma + (q_y - q_{dy}) \cos \gamma,$$

$\mu_1 = \mu_2 = 0.08$ and $q_d = [q_{dx} \ q_{dy}]^T$ is the desired position of the tip of the robot, with $q_{dx} = 2.56$ m and $q_{dy} = 1.8$ m.

Define $e_a \triangleq v - v_d$ and $e_b \triangleq \omega - \omega_d$. Also, define

$$u_{d1}(\hat{\theta}) \triangleq -\phi_4 \hat{\theta} + \frac{1}{1 + \mu_1 + \mu_2} \left(\frac{2\mu_1^2}{l_d} e_2 \dot{e}_2 - (1 + \mu_1 + \mu_2) \dot{e}_1 - K_1 e_a \right),$$

and

$$u_{d2}(\hat{\theta}) \triangleq -\phi_5 \hat{\theta} - \frac{\mu_1}{l_d} \dot{e}_2 - K_2 e_b,$$

where $K_1 = 10$ and $K_2 = 10$.

Hence, the desired control is defined by $u_d(\hat{\theta}) \triangleq [u_{dr}(\hat{\theta}) \ u_{dl}(\hat{\theta})]^T$, where

$$u_{dr}(\hat{\theta}) \triangleq \frac{mrR_a}{2k_m} u_{d1}(\hat{\theta}) + \frac{IrR_a}{2k_ml} u_{d2}(\hat{\theta}),$$

$$u_{dl}(\hat{\theta}) \triangleq \frac{mrR_a}{2k_m} u_{d1}(\hat{\theta}) - \frac{IrR_a}{2k_ml} u_{d2}(\hat{\theta}).$$

If $u(t) = u_d(\theta_*)$, then $\dot{v} = \dot{v}_d - K_1(v - v_d)$ and $\dot{\omega} = \dot{\omega}_d - K_2(\omega - \omega_d)$, which implies that $\lim_{t \rightarrow \infty} v(t) = v_d$ and $\lim_{t \rightarrow \infty} \omega(t) = \omega_d$.

For $i \in \{1, 2\}$, define

$$h_i(x) \triangleq 0.5(q_x - c_{i,1})^2 + 0.5(q_y - c_{i,2})^2 - 0.5(R_i + l_d)^2$$

where $c_{1,1} = 0.65$ m, $c_{1,2} = 0.8$ m, $R_1 = 0.5$, $c_{2,1} = 1.95$ m, $c_{2,2} = 1.75$ m and $R_2 = 0.35$ m describe the physical obstacles, while l_d accounts for the robot's dimension.

The safe set is given by (2), where

$$\psi_0(x) = -\frac{1}{\rho} \log \left(\sum_{i=1}^2 \exp\{-\rho h_i(x)\} \right),$$

and $\rho = 3$ and $d = 2$ [23].

We implement (31)–(35), where $H = 2I_2$, $\beta = 20$ and $\alpha_0 = 5$ and $\alpha_1 = 2$. The control is updated at 200 Hz using a zero-order hold structure.

The cases of the first examples are revisited to analyze and show the impact of the estimate θ and adaptive bound ν in Case 1, and to examine the conservative safety constraint and the degraded performance in Cases 2 and 3.

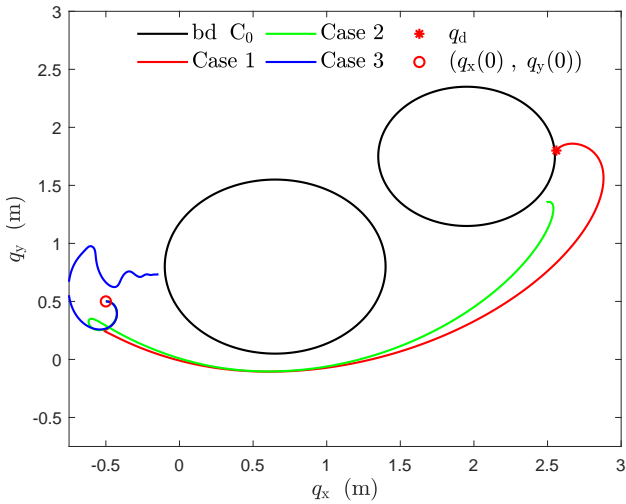


Fig. 6: Phase-Portrait of 3 closed-loop trajectories for Cases 1, 2 and 3.

Figure 6 shows the closed-loop trajectories for $x_0 = [-0.5 \ 0.5 \ 0 \ 0 \ 0]^T$ with a goal at $q_d = [2.56 \ 1.8]^T$ and the cases described above.

Figure 7 shows the states for all 3 cases. Note that only for Case 1, q_x , q_y , v and ω are driven to q_{dx} , q_{dy} , v_d and ω_d . However, in Cases 2 and 3 there is an offset in steady-state between the states and the desired trajectories.

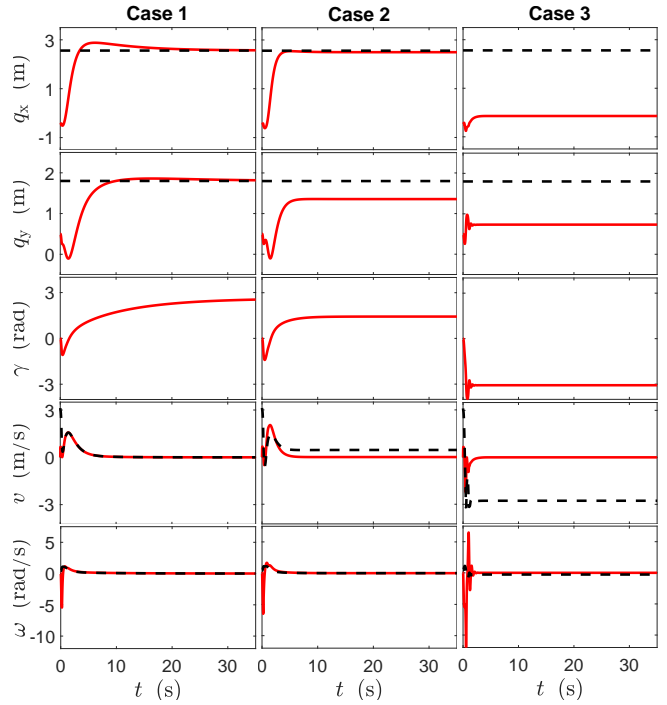


Fig. 7: q_x , q_y , γ , v and ω for Cases 1, 2 and 3. Note that q_{dx} , q_{dy} , v_d and ω_d are shown with dashed lines.

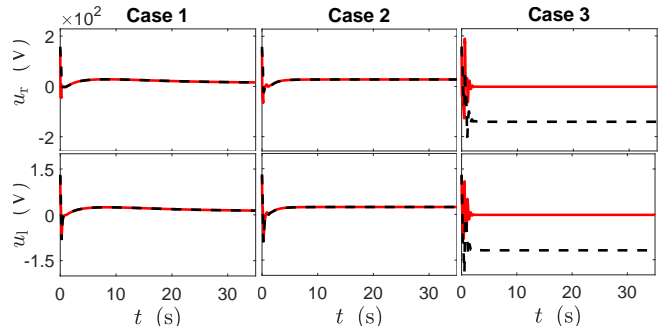


Fig. 8: u_r and u_l for Cases 1, 2 and 3. Note that u_{dr} and u_{dl} are shown with dashed lines.

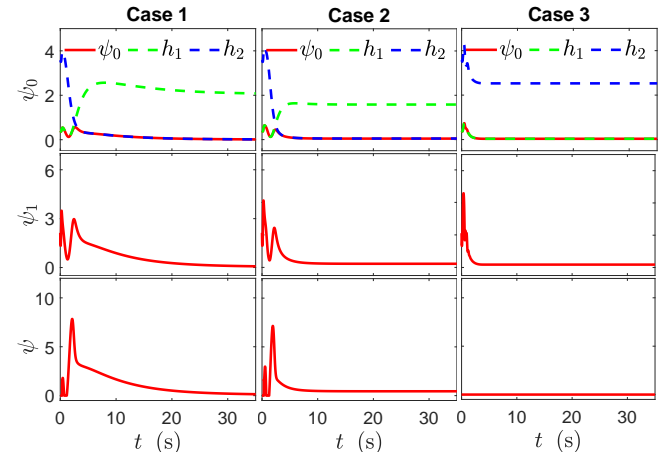


Fig. 9: ψ_0 , ψ_1 and ψ for Cases 1, 2 and 3.

Figure 8 shows that only in Case 3 do the control inputs u_r and u_l not follow the desired controls u_{dr} and u_{dl} .

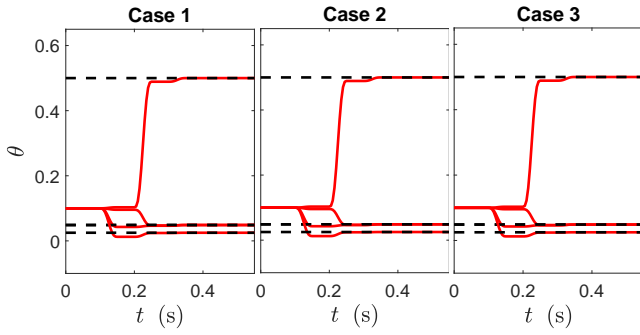


Fig. 10: $\theta(t)$ for Cases 1, 2 and 3. Note that θ_* is shown with dashed lines.

Figure 9 shows that ψ_0 , ψ_1 and ψ are nonnegative, which implies that for all three cases and all $t \geq 0$, $x(t) \in C_0$. In Case 3, for all $t \geq 0$, $\psi(x(t)) = 0$, demonstrating how the conservative safety constraint degrades performance, even as the desired control is adaptively improved.

Figure 10 and 11 show that, for all three cases, $\lim_{t \rightarrow \infty} \theta(t) = \theta_*$ and $\lim_{t \rightarrow \infty} \nu(t) = 0$.

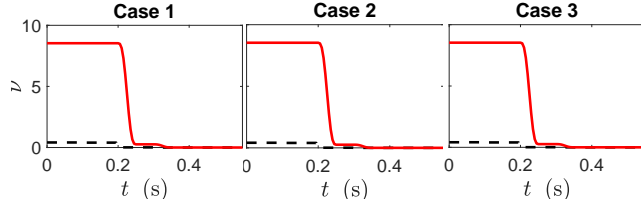


Fig. 11: ν for Cases 1, 2 and 3. Note that $\|\tilde{\theta}_k\|$ is shown with dashed lines.

REFERENCES

- [1] U. Borrmann, L. Wang, A. D. Ames, and M. Egerstedt, "Control barrier certificates for safe swarm behavior," *IFAC-PapersOnLine*, vol. 48, no. 27, pp. 68–73, 2015.
- [2] Z. S. Lippay and J. B. Hoagg, "Formation control with time-varying formations, bounded controls, and local collision avoidance," *IEEE Trans. on Contr. Sys. Tech.*, vol. 30, no. 1, pp. 261–276, 2021.
- [3] C. Heintz, S. C. Bailey, and J. B. Hoagg, "Formation control for autonomous fixed-wing air vehicles with strict speed constraints," *Autonomous Robots*, vol. 47, no. 8, pp. 1299–1323, 2023.
- [4] Q. Nguyen and K. Sreenath, "Safety-critical control for dynamical bipedal walking with precise footstep placement," *IFAC-PapersOnLine*, vol. 48, no. 27, pp. 147–154, 2015.
- [5] F. Borrelli, A. Bemporad, and M. Morari, *Predictive control for linear and hybrid systems*. Cambridge University Press, 2017.
- [6] A. Bemporad, F. Borrelli, M. Morari, et al., "Model predictive control based on linear programming" the explicit solution," *IEEE Trans. Autom. Contr.*, vol. 47, no. 12, pp. 1974–1985, 2002.
- [7] P. Tøndel, T. A. Johansen, and A. Bemporad, "An algorithm for multi-parametric quadratic programming and explicit mpc solutions," *Automatica*, vol. 39, no. 3, pp. 489–497, 2003.
- [8] J. Zeng, B. Zhang, and K. Sreenath, "Safety-critical model predictive control with discrete-time control barrier function," in *Proc. Amer. Contr. Conf.*, pp. 3882–3889, 2021.
- [9] S. Prajna, A. Jadbabaie, and G. J. Pappas, "A framework for worst-case and stochastic safety verification using barrier certificates," *IEEE Trans. Autom. Contr.*, vol. 52, no. 8, pp. 1415–1428, 2007.
- [10] P. Wieland and F. Allgöwer, "Constructive safety using control barrier functions," *IFAC Proceedings Volumes*, vol. 40, no. 12, pp. 462–467, 2007.
- [11] A. D. Ames, X. Xu, J. W. Grizzle, and P. Tabuada, "Control barrier function based quadratic programs for safety critical systems," *IEEE Trans. Autom. Contr.*, vol. 62, no. 8, pp. 3861–3876, 2016.
- [12] Q. Nguyen and K. Sreenath, "Exponential control barrier functions for enforcing high relative-degree safety-critical constraints," in *Proc. Amer. Contr. Conf.*, pp. 322–328, 2016.
- [13] X. Jin, "Adaptive fixed-time control for mimo nonlinear systems with asymmetric output constraints using universal barrier functions," *IEEE Trans. Autom. Contr.*, vol. 64, no. 7, pp. 3046–3053, 2018.
- [14] W. Xiao and C. Belta, "High-order control barrier functions," *IEEE Trans. Autom. Contr.*, vol. 67, no. 7, pp. 3655–3662, 2021.
- [15] X. Tan, W. S. Cortez, and D. V. Dimarogonas, "High-order barrier functions: Robustness, safety, and performance-critical control," *IEEE Trans. Autom. Contr.*, vol. 67, no. 6, pp. 3021–3028, 2021.
- [16] W. Xiao, C. Belta, and C. G. Cassandras, "Event-triggered control for safety-critical systems with unknown dynamics," *IEEE Trans. Autom. Contr.*, vol. 68, no. 7, pp. 4143–4158, 2022.
- [17] J. Breeden and D. Panagou, "Robust control barrier functions under high relative degree and input constraints for satellite trajectories," *Automatica*, vol. 155, p. 111109, 2023.
- [18] Z. Wang, T. Hu, and L. Long, "Multi-uav safe collaborative transportation based on adaptive control barrier function," *IEEE Trans. Sys., Man, and Cyb.: Systems*, 2023.
- [19] Z. Zheng, J. Li, Z. Guan, and Z. Zuo, "Constrained moving path following control for uav with robust control barrier function," *IEEE/CAA Automatica Sinica*, vol. 10, no. 7, pp. 1557–1570, 2023.
- [20] A. D. Ames, S. Coogan, M. Egerstedt, G. Notomista, K. Sreenath, and P. Tabuada, "Control barrier functions: Theory and applications," in *2019 18th Proc. Euro. Contr. Conf.*, pp. 3420–3431, IEEE, 2019.
- [21] R. K. Cosner, A. W. Singletary, A. J. Taylor, T. G. Molnar, K. L. Bouman, and A. D. Ames, "Measurement-robust control barrier functions: Certainty in safety with uncertainty in state," in *2021 IEEE/RSJ Int. Conf. Int. Robots Sys.*, pp. 6286–6291, IEEE, 2021.
- [22] P. Rabiee and J. B. Hoagg, "Soft-minimum and soft-maximum barrier functions for safety with actuation constraints," *Automatica*, 2024.
- [23] P. Rabiee and J. B. Hoagg, "A closed-form control for safety under input constraints using a composition of control barrier functions," *arXiv preprint arXiv:2406.16874*, 2024.
- [24] A. Safari and J. B. Hoagg, "Time-varying soft-maximum barrier functions for safety in unmapped and dynamic environments," *arXiv preprint arXiv:2409.01458*, 2024.
- [25] M. Jankovic, "Robust control barrier functions for constrained stabilization of nonlinear systems," *Automatica*, vol. 96, pp. 359–367, 2018.
- [26] M. H. Cohen, C. Belta, and R. Tron, "Robust control barrier functions for nonlinear control systems with uncertainty: A duality-based approach," in *Proc. Conf. Dec. Contr.*, pp. 174–179, IEEE, 2022.
- [27] A. J. Taylor and A. D. Ames, "Adaptive safety with control barrier functions," in *Proc. Amer. Contr. Conf.*, pp. 1399–1405, IEEE, 2020.
- [28] B. T. Lopez, J.-J. E. Slotine, and J. P. How, "Robust adaptive control barrier functions: An adaptive and data-driven approach to safety," *IEEE Contr. Syst. Letts.*, vol. 5, no. 3, pp. 1031–1036, 2020.
- [29] Q. Nguyen and K. Sreenath, "L1 adaptive control barrier functions for nonlinear underactuated systems," in *Proc. Amer. Contr. Conf.*, pp. 721–728, 2022.
- [30] M. H. Cohen and C. Belta, "High order robust adaptive control barrier functions and exponentially stabilizing adaptive control lyapunov functions," in *Proc. Amer. Contr. Conf.*, pp. 2233–2238, IEEE, 2022.
- [31] D. Zeng, Y. Jiang, Y. Wang, H. Zhang, and Y. Feng, "Robust adaptive control barrier functions for input-affine systems: Application to uncertain manipulator safety constraints," *IEEE Contr. Syst. Letts.*, 2023.
- [32] A. A. Ali, J. B. Hoagg, M. Mossberg, and D. S. Bernstein, "On the stability and convergence of a sliding-window variable-regularization recursive-least-squares algorithm," *Int. J. of Adap. Contr. Sig. Process.*, vol. 30, no. 5, pp. 715–735, 2016.
- [33] W. S. Cortez and D. V. Dimarogonas, "On compatibility and region of attraction for safe, stabilizing control laws," *IEEE Trans. Autom. Contr.*, vol. 67, no. 9, pp. 4924–4931, 2022.
- [34] I. Anvari, "Non-holonomic differential drive mobile robot control & design: Critical dynamics and coupling constraints," tech. rep., Arizona State University, 2013.